

Seasonal variation in energy balance and canopy conductance for a tropical savanna ecosystem of south central Mato Grosso, Brazil

Thiago R. Rodrigues,¹ George L. Vourlitis,² Francisco de A. Lobo,³
Renan G. de Oliveira,⁴ and José de S. Nogueira¹

Received 5 August 2013; revised 19 November 2013; accepted 23 November 2013.

[1] Tropical savanna (locally known as cerrado) composes 24% of Brazil and is characterized by high climatic variation; however, patterns of energy exchange are poorly understood, especially for mixed grasslands (locally known as *campo sujo*). We used eddy covariance to measure latent (L_e) and sensible (H) heat flux of a mixed grassland and linked meteorological and remote sensing data to determine the controls on these fluxes. We hypothesized that (1) seasonal variations in H and L_e would be large due to variations in precipitation; (2) ecosystem phenology, estimated using the enhanced vegetation index (EVI), would be the best predictor of seasonal variation in L_e ; and (3) cerrado, transitional, and humid evergreen forests would have similar rates of average annual L_e despite large seasonal variation in cerrado L_e . Our data suggest that *campo sujo* exhibits large seasonal fluctuations in energy balance that are driven by rainfall and that responses to rainfall pulses are rapid and dynamic, especially during the dry season. Path analysis indicated that temporal variations in the EVI did not significantly affect L_e or G_c , but this was because all three variables (EVI, L_e , and G_c) responded similarly to temporal variations in surface water availability. Compared to other tropical ecosystems, wetter sites had higher rates of L_e during the dry season but similar rates during the wet season when water was not limiting. Over annual time periods, average rates of L_e increased significantly as average annual rainfall increased, due to dry-season water limitations in the more seasonal tropical ecosystems.

Citation: Rodrigues, T. R., G. L. Vourlitis, F. d. A. Lobo, R. G. de Oliveira, and J. d. S. Nogueira (2014), Seasonal variation in energy balance and canopy conductance for a tropical savanna ecosystem of south central Mato Grosso, Brazil, *J. Geophys. Res. Biogeosci.*, 119, doi:10.1002/2013JG002472.

1. Introduction

[2] Tropical savannas cover about 12% of the global land surface [Scholes and Archer, 1997] and are characterized by high plant species diversity [Giambelluca *et al.*, 2009]. In Brazil, savanna (locally known as cerrado) covers about 24% of the country and is the dominant vegetation in areas subjected to a prolonged dry season [Lascano, 1991; San José *et al.*, 1998; Rodrigues *et al.*, 2011, 2013].

[3] Cerrado has been heavily impacted by human activities over the last four to five decades, in particular, conversion to cattle pasture and soybean and sugarcane production [Klink

and Moreira, 2002; Giambelluca *et al.*, 2009] and has experienced higher rates of deforestation than tropical forest in the Amazon Basin [Mueller, 2003]. In general, these anthropogenic activities increase fire frequency and decrease the woody vegetation [Oliveira *et al.*, 2005], converting vegetation to a more open, grass-dominated, and shallow-rooted ecosystem. These changes significantly affect atmospheric properties and processes, such as boundary layer dynamics [Niyogi *et al.*, 1999; Baidya Roy and Avissar, 2002], convection [Pielke, 2001], cloudiness and cloud properties [Ray *et al.*, 2003], and precipitation [Foley *et al.*, 2003; Pielke *et al.*, 2007; Douglas *et al.*, 2009]. Forest conversion to pasture in tropical systems can cause increases in vapor pressure deficit and surface temperature [Culf *et al.*, 1996], increase the duration of the dry season, and cause more rainfall to be partitioned into runoff [Von Randow *et al.*, 2004; Costa and Pires, 2010].

[4] While human activities have been more extensive, cerrado has received relatively little attention from researchers in comparison with tropical rain forests [Von Randow *et al.*, 2004; Fisher *et al.*, 2008; Zeri and Sá, 2010]. Past work in the cerrado has characterized the mass (CO_2 and H_2O vapor) and energy balance [Miranda *et al.*, 1997; da Rocha *et al.*, 2002, 2009; Santos *et al.*, 2003; Oliveira *et al.*, 2005; Sanches *et al.*, 2011; Rodrigues *et al.*, 2013], but cerrado structure is complex, ranging from dense and tall forests (*Cerradão*), mixed

¹Programa de Pós Graduação em Física Ambiental, Instituto de Física, Universidade Federal de Mato Grosso, Cuiabá, Brazil.

²Biological Sciences Department, California State University, San Marcos, California, USA.

³Departamento de Agronomia e Medicina Veterinária, Universidade Federal de Mato Grosso, Cuiabá, Brazil.

⁴Instituto Federal de Educação, Ciência e Tecnologia de Mato Grosso, Sorriso, Brazil.

Corresponding author: G. L. Vourlitis, Biological Sciences Department, California State University, San Marcos, CA 92096, USA.
(georgev@csusm.edu)

©2013. American Geophysical Union. All Rights Reserved.
2169-8953/14/10.1002/2013JG002472



Figure 1. Location of the study site near Cuiabá-MT and locations of other study sites where latent heat flux (L_e) data were used for a comparison between values measured here and across a rainfall gradient in Brazil. Site locations are listed in Table 2, and symbols correspond to Amazonia forests (closed circles), transitional forests (open circles), and cerrado (inverted, closed triangles).

woodlands (*sensu stricto*), and grass-dominated ecosystems with (*campo sujo*) and without (*campo limpo*) trees and shrubs [Eiten, 1972; Furley and Ratter, 1988]. These structural variations have the potential to cause large spatial and temporal variations in energy flux partitioning; however, most of the work done in cerrado has come from forest and woodland systems [Miranda et al., 1997; da Rocha et al., 2002, 2009; Sanches et al., 2011]. Thus, our goals were to characterize the seasonal variation in energy balance for a grass-dominated cerrado ecosystem, determine the seasonal controls on these energy fluxes, and to compare our results with those published for other tropical ecosystems to see if there are patterns in energy flux across regional rainfall gradients. We hypothesize that (1) seasonal variations in sensible (H) and latent (L_e) heat flux will be large due to seasonal variations in precipitation, (2) seasonal variations in ecosystem phenology, estimated from the enhanced vegetation index (EVI) derived from Moderate Resolution Imaging Spectroradiometer (MODIS), will be the best predictor of seasonal variations in L_e , and (3) cerrado, transitional, and humid evergreen forests will have similar rates of average annual L_e despite large seasonal variation in cerrado L_e .

2. Methods

2.1. Site Description

[5] The study was conducted in the Cuiabá Basin at the Fazenda Miranda (FM), located 15 km SSE of Cuiabá, Mato Grosso, Brazil (Figure 1). The study site was a mixed forest-grassland (locally known as *campo sujo* or “dirty field”) that was partially cleared of trees approximately 35 years ago. Vegetation consists predominately of grasses and the tree species *C. americana* and *Diospyros hispida* A. DC. According to Koppen, the climate of region is characterized as Aw, tropical

semihumid, with dry winters and wet summers. Mean annual rainfall and temperature are 1420 mm and 26.5°C, respectively, and rainfall is seasonal with a dry season extending from May–September [Vourlitis and da Rocha, 2011]. The range of mean monthly air temperature is wide relative to transitional and humid evergreen tropical forests, with a minimum of 23.5°C in June and a maximum of 28.6°C in September [Vourlitis and da Rocha, 2011]. The research area is on flat terrain at an elevation of 157 m above sea level. The regional soil type is a rocky, dystrophic red-yellow latosol locally known as a Solo Concrecionário Distrófico [Radambrasil, 1982].

2.2. Micrometeorological Measurements

[6] Micrometeorological and eddy covariance measurements were conducted between March 2011 and 2012. A micrometeorological tower enabled the collection of data on air temperature (T_a), relative humidity (RH), wind speed (u), precipitation (P), soil temperature (T_s), soil heat flux (G), net radiation (R_n), solar radiation (R_s), soil moisture (SH_2O), latent heat flux (L_e), and sensible heat flux (H). T_a and RH were measured 10 m above the ground level using a thermohygrometer (HMP45AC, Vaisala Inc., Woburn, MA, USA). Wind speed was measured 10 m above the ground level using anemometer (03101 R. M. Young Company), and G was measured using heat flux plates (HFP01-L20, Hukseflux Thermal Sensors BV, Delft, Netherlands) installed 1.0 cm below the soil surface ($n=2$), with one placed in a sandy soil type and the other placed in a laterite soil type, which were typical of the local soil in the tower footprint. Soil moisture (SH_2O) was measured using time domain reflectometry probes installed 20 cm below the soil surface ($n=2$), placed in the two soil types described above (CS616-L50, Campbell Scientific, Inc., Logan, UT, USA). R_n and R_s were measured

5 m aboveground using a net radiometer (NR-LITE-L25, Kipp & Zonen, Delft, Netherlands) and a pyranometer (LI200X, LI-COR Biosciences, Inc., Lincoln, NE, USA), respectively. Precipitation was measured using a tipping bucket rainfall gauge (TR-525M, Texas Electronics, Inc., Dallas, TX, USA). The sensors were connected to a data logger (CR1000, Campbell Scientific, Inc., Logan, UT, USA) that scanned each sensor every 30 s and stored average, and in the case of P , total quantities every 30 min.

[7] Latent (L_e) and sensible heat flux (H) were quantified using eddy covariance. Eddy covariance sensors were mounted at a height of 10 m above ground level or 8–8.5 m above the shrub canopy. Wind direction was typically out of the NNW and NNE, and analysis of the upwind distance sampled by the eddy covariance system (fetch) estimated using the model by Schuepp *et al.* [1990] indicated that about 90% of the flux originated within 1 km upwind of the tower.

[8] The eddy covariance system consisted of a 3-D sonic anemometer-thermometer (CSAT-3, Campbell Scientific, Inc., Logan, UT, USA) to measure the mean and fluctuating quantities of wind speed and temperature and an open-path infrared gas analyzer (LI-7500, LI-COR, Inc., Lincoln, NE, USA) to measure the mean and fluctuating quantities of H_2O vapor. Both sensors sampled and output data at 10 Hz and were oriented in the direction of the mean wind. Raw (10 Hz) data and 30 min average fluxes were stored and processed using a solid-state data logger (CR1000, Campbell Scientific, Inc., Logan, UT, USA).

[9] Average fluxes of L_e and H were obtained by calculating the covariance between the fluctuations in vertical wind speed and H_2O vapor density and temperature, respectively, over a 30 min interval following a coordinate rotation of the wind vectors [McMillen, 1988]. Water vapor flux was corrected for the simultaneous fluctuations in heat following Webb *et al.* [1980].

2.3. Canopy Conductance Calculation

[10] Canopy conductance (G_c) was calculated during daytime periods (0800–1600 h local time) from micrometeorological and eddy covariance data using the inverted Penman-Monteith equation [Monteith, 1981; Dolman *et al.*, 1991; Harris *et al.*, 2004],

$$G_c = G_a \left[\frac{(\Delta Q + \rho C_p D G_a)}{\gamma L_e} \quad \frac{\Delta}{\gamma} \quad 1 \right]^{-1} \quad (1)$$

where G_a is the aerodynamic conductance (m s^{-1} ; described below), Δ is the slope of the saturation vapor pressure versus temperature curve (kPa/K), ρ is the density of dry air (g m^{-3}), C_p is the specific heat capacity ($\text{J g}^{-1} \text{K}^{-1}$), D is the atmospheric vapor pressure deficit (kPa), γ is the psychrometric constant (kPa K^{-1}), and Q is the available energy calculated as $R_n - G$ ($\text{J m}^{-2} \text{s}^{-1}$).

[11] Aerodynamic conductance, G_a (m s^{-1}), was calculated (equation 2),

$$G_a = \frac{u^2}{u^*} \quad (2)$$

where u =wind speed measured from the triaxial sonic anemometer and u^* =frictional velocity calculated from eddy covariance measurements of momentum flux [Baldocchi *et al.*, 1991].

[12] The average daytime (0800–1600 h) decoupling coefficient (Ω) was calculated according to Jarvis and McNaughton [1986],

$$\Omega = \left[1 + \frac{\gamma}{\Delta + \gamma} \frac{r_c}{r_a} \right]^{-1} \quad (3)$$

where r_c is the canopy resistance (s/m) and r_a is the aerodynamic resistance (s/m), which are the inverse of canopy and aerodynamic conductance, respectively. Values of Ω vary between 0 and 1, and values approaching zero indicate that the canopy is more coupled to the overlying atmosphere [Jarvis and McNaughton, 1986]. In tall, aerodynamically rough canopies such as forests and/or woodlands, G_a typically exceeds G_c , and the canopy is more aerodynamically coupled with the overlying atmosphere. Under these conditions, variations in G_c and L_e may be more sensitive to variations stomatal conductance (g_s) and D than in shorter, aerodynamically smooth canopies such as grasslands [Jarvis and McNaughton, 1986; Jones, 1992].

2.4. Spectral Reflectance Measurements

[13] Time series of the 250 m resolution, 16 day MODIS enhanced vegetation index (EVI) composites (Land Products, Collection 5, C5_MOD13Q1) were obtained for the tower site from the Oak Ridge National Laboratory [Oak Ridge National Laboratory-Distributed Active Archive Center, 2013]. EVI values were averaged for the 4 pixels partially covering the eddy flux tower. The MOD13Q1 pixel reliability band was used to filter the EVI data and only the highest quality pixel quartets were retained. Data gaps in the EVI time series due to low pixel quality and/or infrequent (16 day) sampling were filled using autoregressive integrated moving average models [Edwards and Coull, 1987; Vourlitis *et al.*, 2008].

2.5. Data Analysis

[14] Path analysis was used to evaluate the direct and indirect effects of microclimate (P , R_n , SH_2O , D) and the EVI on L_e and G_c [Sokal and Rohlf, 1995; Huxman *et al.*, 2003]. This method is similar to multiple regression but is more appropriate when relationships between variables are either known or hypothesized and/or when the statistical independence between variables is uncertain [Sokal and Rohlf, 1995]. To calculate path values we developed five multiple regression models (Figure 2), where (1) L_e or $G_c = f$ (average weekly P , T_a , R_n , D , SH_2O , and EVI), (2) $R_n = f$ (average weekly P), (3) $\text{EVI} = f$ (average weekly R_n , D , and SH_2O), (4) $D = f$ (average weekly P , T_a , and SH_2O), and (5) $\text{SH}_2\text{O} = f$ (average weekly P , R_n , and T_a). Partial least squares analysis was used to quantify the standardized partial regression coefficient for each independent variable. Direct effects of average weekly R_n , EVI, VPD, and SH_2O on L_e or G_c were estimated as the standardized partial regression coefficients quantified from model 1, while indirect effects of other variables were quantified as the product of the standardized partial regression coefficients summed across each possible path [Huxman *et al.*, 2003].

[15] Daily averages and/or totals were summarized as mean ($\pm \text{sd}$) values calculated over weekly intervals unless specified. Diel (24 h) averages of energy flux density, micrometeorology, and conductance were calculated over seasonal intervals by averaging each 30 min datum for a particular

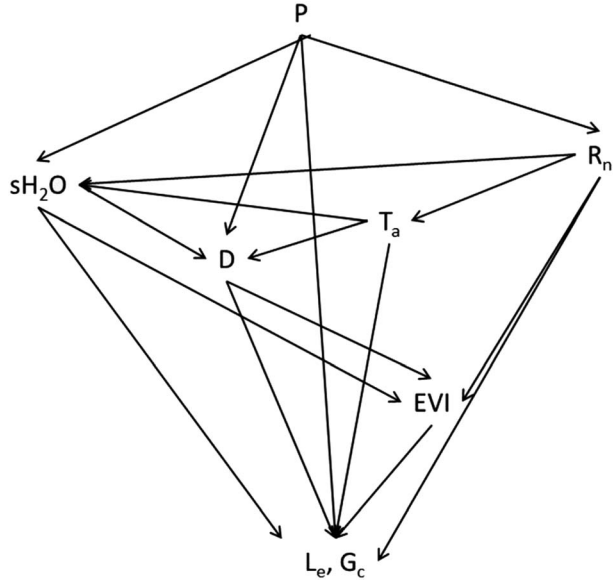


Figure 2. Path diagram of the direct and indirect effects of average weekly precipitation (P), net radiation (R_n), soil moisture content (SH_2O), air temperature (T_a), vapor pressure deficit (D), and the enhanced vegetation index (EVI) on average weekly latent heat flux (L_e) and canopy conductance (G_c).

time (e.g., 0800–0830 h). Sensor and/or infrastructure failures caused gaps in data collection, and short-term events such as intense rainfall led to the rejection of data. Gaps were filled using linear regression where the missing data series (i.e., R_n , L_e , and H) was estimated from a similar variable (i.e., R_s). These gaps accounted for < 5% of the total possible measurements during the study period.

3. Results and Discussion

3.1. Eddy Covariance System Performance

[16] System performance was assessed by linear regression of the energy balance closure with the sum of sensible plus latent heat flux ($H+L_e$) measured from eddy covariance as the dependent variable and the difference between net radiation and ground heat flux (R_n-G) measured from the meteorological sensors as the independent variable [McMillen, 1988]. Instantaneous (30 min average) measurements $H+L_e$ accounted for only about 75% of R_n-G ($R^2=0.89$; $n=17,230$), and there was a significant y intercept (Figure 3). Thus, the eddy covariance data tended to underestimate the net energy loss at night and the net energy gain during the day, but the degree of closure is comparable to that reported for other temperate and tropical forest eddy covariance systems [Aubinet et al., 2000; Araújo et al., 2002; Malhi et al., 2002; Vourlitis et al., 2008; Giambelluca et al., 2009]. To assess the potential for short-term variation in energy storage, energy balance closure was also assessed using daily averages of $H+L_e$ and R_n-G . However, the degree of energy balance closure did not change when average daily values were used (Figure 3b), suggesting that instantaneous variations in energy storage were negligible. This result is in contrast to those reported for taller, denser, tree-dominated tropical ecosystems [Araújo et al., 2002; Malhi et al., 2002; Vourlitis et al., 2008; Giambelluca et al.,

2009] and likely reflects the grass-dominated structure of the *campo sujo* cerrado studied here.

3.2. Seasonal Variations in Micrometeorology and Spectral Reflectance

[17] The climate of the study area is highly affected by the seasonal variation in rainfall (Figure 4). Approximately 93% of the recorded rainfall occurred between the months of November and April (i.e., the wet season), with only sporadic rainfall during the dry-season months of May–October (Figure 4a). This pattern of rainfall is typical for this region [Vourlitis and da Rocha, 2011]. Some months, such as March 2011, had extremely high rainfall that exceeded 330 mm, while other months, such as May, July, and August, had no measurable rainfall (Figure 4a). Total accumulated rainfall was 1030 mm during the study period, which was on average 27% lower than the long-term average for this region [Vourlitis and da Rocha, 2011]. Assuming that the dry season can be defined as the number of months with rainfall less than 100 mm/month [Hutyra et al., 2005]. The dry-season duration for the study period spanned 6 months (May–October), which is approximately 1 month longer than the long-term average [Vourlitis and da Rocha, 2011].

[18] Trends in surface soil moisture (0–20 cm) followed trends in rainfall closely, but changes in soil moisture in response to rainfall pulses were much more pronounced during the dry season (Figure 4a). Maximum values of percent

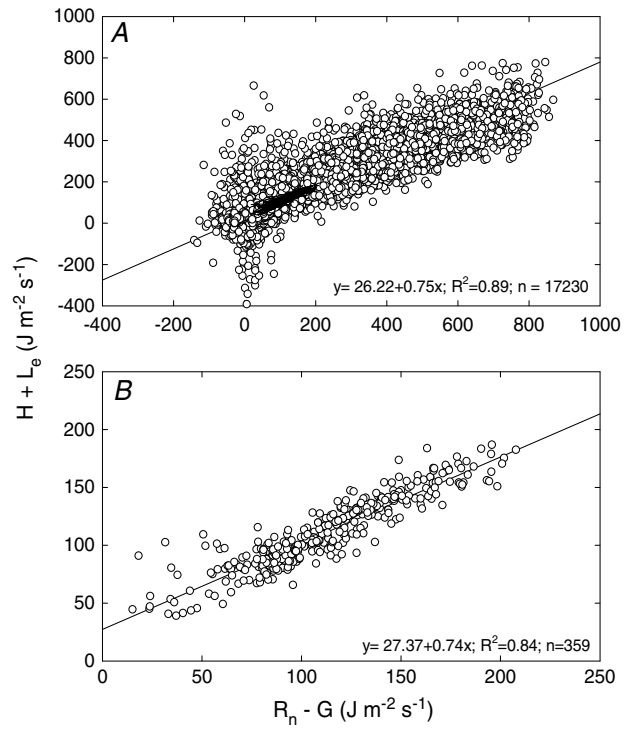


Figure 3. Energy balance closure for (a) 30 min average values and (b) average daily values of latent plus sensible heat flux ($H+L_e$; dependent variable) versus net radiation minus ground heat flux (R_n-G ; independent variable). Also shown are the linear regression results including the equation of best fit, coefficient of determination (R^2), and the number of samples included in the regression.

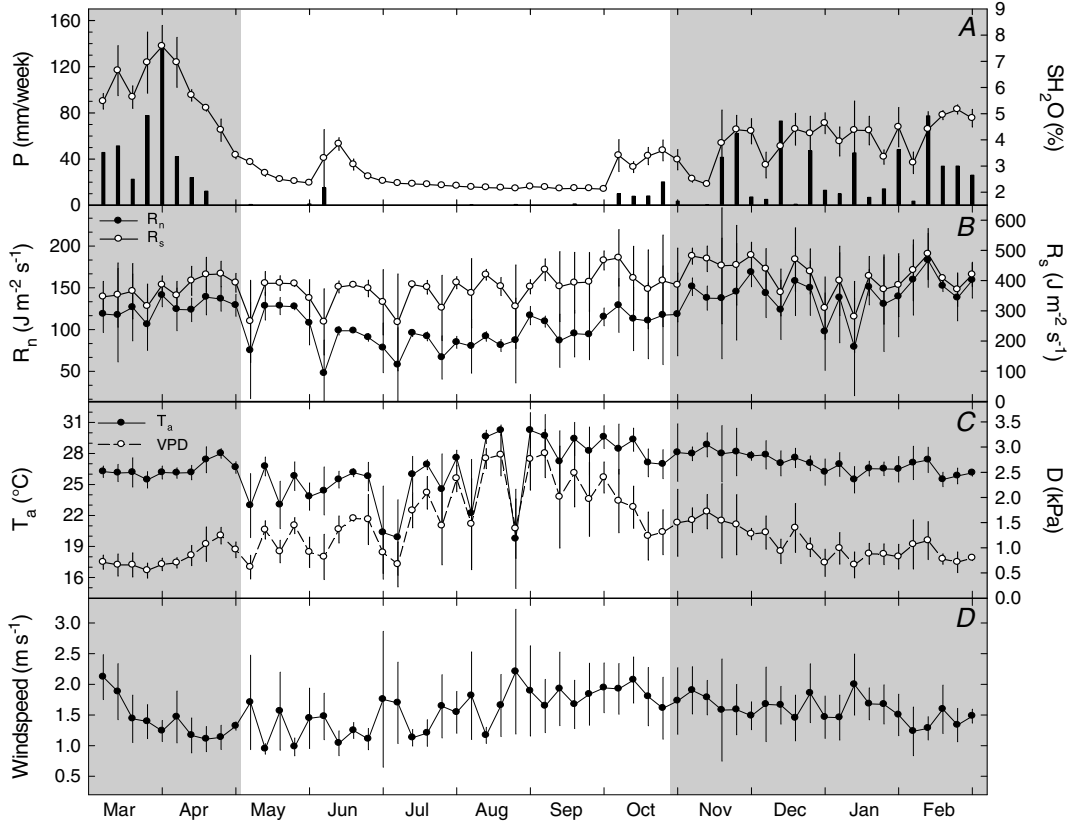


Figure 4. (a) Total weekly precipitation (bars, left-hand axis) and average weekly (\pm sd) surface soil moisture (white circles, right-hand axis), (b) average weekly (\pm sd) net radiation (R_n ; black circles, left-hand axis) and incident solar radiation (R_s ; white circles, right-hand axis), (c) air temperature (T_a ; black circles, left-hand axis) and vapor pressure deficit (D ; white circles, right-hand axis), and (d) wind speed during the study period. Shaded portions indicate the wet season.

gravimetric soil moisture (mass water/mass dry soil) were only on the order of 9%, which is likely due to the coarse, rocky nature of the soil type that is common to the Cuiaba Basin [Radambrasil, 1982]. Vourlitis *et al.* [2013] reported that the soil was sandy (70% by weight) and rocky (65% by weight), and these soils have very rapid infiltration rates but little water holding capacity [Teepe *et al.*, 2003], which causes large fluctuations in soil moisture in response to rainfall pulses. During the wet season, average weekly percent soil moisture ranged between 5 and 8%, while during the dry season, soil water content was as low as 2.1% for several weeks when rainfall was either scarce or too low to measure (Figure 4a). However, two dry-season periods are noteworthy, one that occurred in the first week of June and another that occurred in the month of October, when rainfall events caused large but transient increases in soil moisture (Figure 4a). Once into the wet season, other rainfall pulses, such as the one observed during the third and fourth weeks of November lead to similar short-term increases in soil moisture; however, wet season variations in soil moisture were smaller than the dry-season pulses described above.

[19] Net radiation was typically higher during the wet season than during the dry season, although relatively larger standard deviations during the wet season indicate large day-to-day variations in R_n (Figure 4b) when there is frequent cloud cover [Machado *et al.*, 2004]. This pattern is typical of the cerrado biome but is opposite to that observed for the

humid evergreen forest of the Amazon Basin where prolonged cloud cover tends to reduce wet-season R_n [da Rocha *et al.*, 2009]. The seasonal pattern for R_s was less pronounced than the seasonal pattern of R_n , and in general, the highest values were observed in October–November during the dry-wet season transition (Figure 4b). These data suggest that the dry-season decline in R_n was due in part to an increase in the surface albedo caused by a decline in vegetation leaf area and/or greenness during the dry season when soil water availability was low [Machado *et al.*, 2004; Ratana *et al.*, 2005; Rodrigues *et al.*, 2013].

[20] Temporal fluctuations in T_a (Figure 4c) were substantially smaller during the wet season compared to the dry season, when frequent cold fronts that originate in southern Brazil [Grace *et al.*, 1996] caused T_a to fluctuate by as much as 10°C from week to week. During the study period, the mean (\pm sd) temperature was $26.3 \pm 2.1^\circ\text{C}$, and the period of the lowest average T_a was in June ($23.5 \pm 3.1^\circ\text{C}$), while the period with the highest average T_a was in September ($28.6 \pm 0.9^\circ\text{C}$). Weekly trends in the atmospheric vapor pressure deficit (D) also varied over seasonal scales, with the lowest average D (0.4–0.7 kPa) observed during the wet season and the highest (2.5–3.0 kPa) observed during the dry season in August and September (Figure 4c). These seasonal variations are high compared to transitional tropical forests [Vourlitis *et al.*, 2008] and humid tropical forests of the Amazon Basin [Culf *et al.*, 1996; da Rocha *et al.*, 2004] but

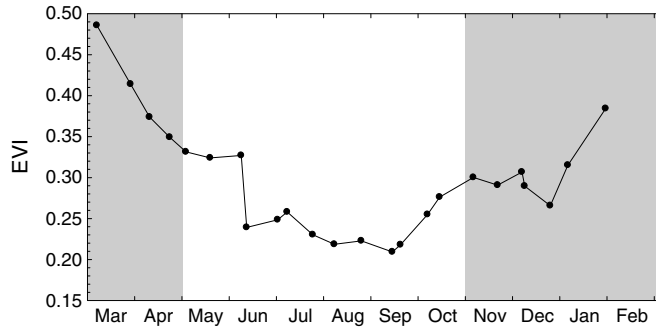


Figure 5. Average enhanced vegetation index (EVI) calculated from 16 day composites for pixels encompassing the eddy flux tower footprint. Shaded portions indicate the wet season.

similar to tropical savannas of central Brazil [Giambelluca *et al.*, 2009].

[21] Wind speed did not exhibit consistent seasonal variations and was on average (\pm sd) $1.5 \pm 0.3 \text{ m s}^{-1}$ during the study period (Figure 4d). Relatively large day-to-day variations were evident, which is typical of the sporadic nature of wind speed in this region [Biudes, 2008].

[22] Seasonal trends in the EVI were large (Figure 5) and reflected the seasonal variation in the distribution of rainfall and soil water availability (Figure 4a). For example, the EVI was positively correlated with rainfall ($r=0.80$; $p < 0.001$) and SH_2O ($r=0.57$; $p < 0.001$), which is consistent with observations from other cerrado sites near Brasilia [Ratana *et al.*, 2005]. However, in contrast to Ratana *et al.* [2005], there was no 1–2 month lag in the response of the EVI to seasonal variations in rainfall or SH_2O .

[23] EVI was highest in March at the beginning of the study period but declined consistently into the dry season. The March–April decline in the EVI occurred despite the 411 mm of rainfall recorded during this period (Figure 4a) and is likely attributed to leaf abscission that occurs during the wet-dry season transition for many cerrado tree species as D begins to increase [Lenza and Klink, 2006; Silvério and Lenza, 2010; Dalmagro *et al.*, 2013]. Minimum values of the EVI were observed during the peak of the dry season (August–September), but EVI increased in late September and into October, approximately 4 weeks prior to the end of the dry season (Figure 5). This seasonal pattern is consistent with other cerrado sites [Machado *et al.*, 2004; Ratana *et al.*, 2005], reflecting the importance of the rainfall distribution on leaf expansion and productivity in cerrado. Spectral reflectance (EVI and the NDVI) indicates that tree- and grass-dominated cerrado has the same phenology in response to rainfall; however, the dynamic range of grass-dominated cerrado is larger than tree- and shrub-dominated cerrado because cerrado grasses have a lower dry-season minimum than trees and shrubs [Ratana *et al.*, 2005]. During the dry-wet season transition, increases in rainfall have been shown to increase the leaf production and expansion for both cerrado grasses and trees [Mantovani and Martins, 1988; Lenza and Klink, 2006; Silvério and Lenza, 2010]. Furthermore, many cerrado trees exhibit a flush of new leaves at the end of the dry season that is supported by internal water reserves [Mantovani and Martins, 1988; Lenza and Klink, 2006; Silvério and Lenza, 2010]. These phenological patterns are in contrast to those reported for Amazonian forests, which exhibit periods of leaf production and expansion during the wet-dry

season transition, because productivity is primarily light limited in Amazonian forests but water limited in cerrado [Machado *et al.*, 2004; Saleska *et al.*, 2009].

3.3. Average Diel Trends in Energy Flux Density and Conductance

[24] Diel averages of R_n , H , L_e , and G calculated for each month exhibited large variations over the study period (Figure 6a). Regardless of the month, R_n reached a peak at 1200 local time while trends in L_e , H , and G followed closely. However, the relative peaks in energy fluxes varied substantially over the study period based on rainfall and water availability. For example, during the wet season, midday peaks in L_e were on the order of 2–4 times higher than H and G (Figure 6a), and L_e accounted for up to 50% of the available energy (R_n). However, during the dry season, peaks in L_e and G were comparable, while H was the dominant pathway of energy dissipation (Figure 6a). H accounted for up to 50% of R_n during the peak of the dry season (September), while G accounted for nearly 30% of R_n during the same period. Such a contribution of G during the dry season is in contrast to other tropical ecosystems such as tropical and transition forests, where G accounts for only 1–2% of the available energy and likely reflects the more open canopy of *campo sujo* cerrado and the senescence of grasses and other vegetation during the long dry season [Giambelluca *et al.*, 2009]. These seasonal variations in energy flux occurred abruptly during the season transitions and reflect the importance of surface water availability in controlling energy fluxes in seasonal tropical ecosystems [Miranda *et al.*, 1997; Oliveira *et al.*, 2005; da Rocha *et al.*, 2009; Vourlitis and da Rocha, 2011; Rodrigues *et al.*, 2013].

[25] Mean daytime (0800–1600 h local time) canopy conductance (G_c ; Figure 6b) also displayed large seasonal variation. In general, G_c exhibited maximum values in the morning, declined during the midday (1000–1400 h local time), and increased again during the late afternoon. This pattern was apparent even during the wet season, when soil water availability was high (Figure 4a) and midday L_e was at a maximum (Figure 6a). The consistent midday decline in G_c was likely due to the midday increase in temperature and the vapor pressure deficit (D) [Malhi *et al.*, 2002; Vourlitis *et al.*, 2008; Giambelluca *et al.*, 2009]. However, daytime maxima and minima varied substantially over the study period, with the highest values during the wet season and the lowest values during the dry season, and minimum midday values of G_c during the wet season were often higher

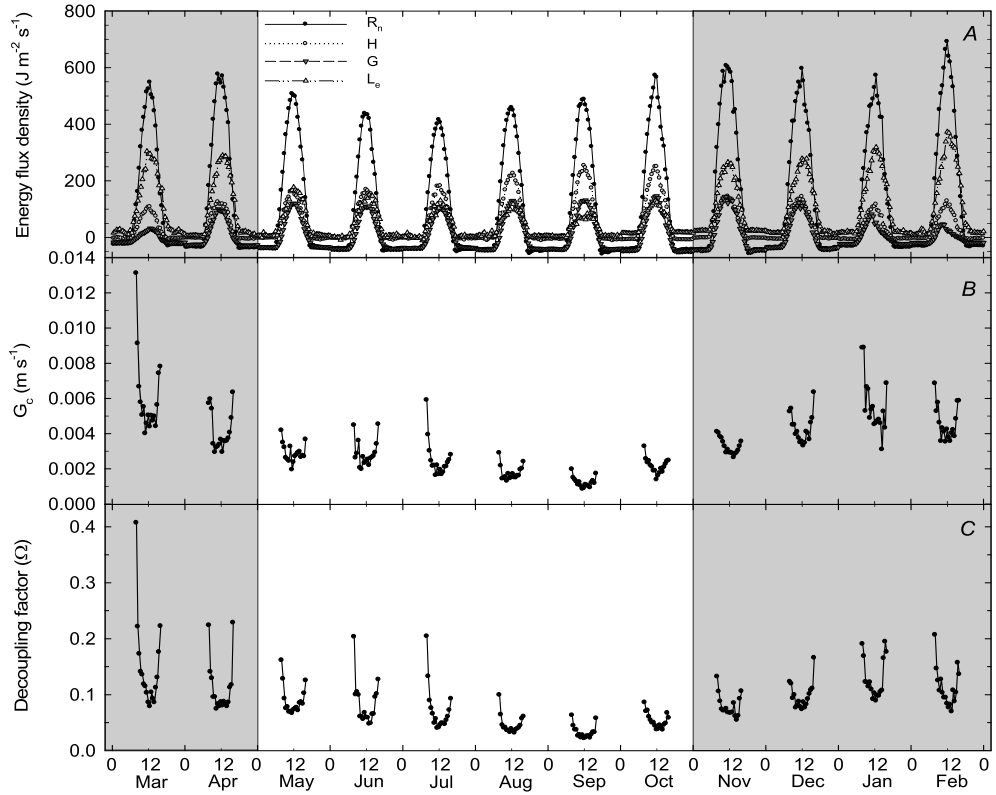


Figure 6. (a) Average diel trends in net radiation (R_n ; black circles), latent heat (L_e ; white triangles), sensible (H ; white circles), and ground heat flux (inverted triangles) and average daytime (0900–1500 h local time) (b) Canopy conductance and (c) the decoupling factor calculated for each month of the study period.

than maximum values of G_c observed during the dry season (Figure 6b). Diel values of G_c declined into the dry season and began to increase in October during the dry-wet season transition when rainfall lead to an increase in surface evaporation and the EVI (Figure 5). By the beginning of the wet season in November, midday rates of G_c were steadily increasing, which was coincident with an increase in soil water content (Figure 4a), a decline in the D (Figure 4c) and an increase in the EVI.

[26] Diel values of Ω were highest during the early morning and late afternoon (Figure 6c) when wind speed and aerodynamic conductance (G_a) were low (data not shown). However, midday values of Ω were consistently < 0.12 (Figure 6c), indicating tight coupling between the vegetation and the atmosphere and potentially strong stomatal control on G_c [Jarvis and McNaughton, 1986; Jones, 1992], even during the wet season when soil water availability and precipitation were adequate to promote high values of midday L_e (Figure 6a). This result is somewhat surprising given that *campo sujo* is a grass-dominated ecosystem, which is typically aerodynamically smooth and is relatively less coupled to the atmosphere than forests and woodlands [Jarvis and McNaughton, 1986; Jones, 1992]. However, *campo sujo* has scattered trees and shrubs [Eiten, 1972], and at Fazenda Miranda, *campo sujo* has a woody density of 533 trees/ha [Vourlitis et al., 2013], which is apparently adequate to promote high G_a and thus, low values of Ω . Our results are similar to those reported for other mixed grassland-woodland savanna sites [Bagayoko et al., 2007], indicating that tree-grass mixtures can be highly coupled to the atmosphere. Because of the high degree of

surface-atmosphere coupling (i.e., low Ω), midday declines in G_c were probably due to declines in stomatal conductance that were caused by a high D [Jarvis and McNaughton, 1986; Jones, 1992]. This interpretation is consistent with other studies from cerrado [Giambelluca et al., 2009] and from measurements of stomatal conductance for a variety of cerrado trees [Bucci et al., 2008; Vourlitis and da Rocha, 2011; Dalmagro et al., 2013].

3.4. Seasonal Trends in Energy Flux Density and Conductance

[27] Temporal variations in average weekly L_e were large during the study period, especially during the wet-dry and dry-wet season transitions (Figure 7a). The decline in L_e during the wet-dry transition was approximately 65% of the wet-season values, with a mean ($\pm \text{sd}$) L_e on the order of $100.8 \pm 12.7 \text{ J m}^{-2} \text{ s}^{-1}$ during the wet season to a mean of $43.1 \pm 9.1 \text{ J m}^{-2} \text{ s}^{-1}$ during the dry season. Transient variations in L_e were observed during the dry season, and in general, L_e increased rapidly in response to small and infrequent rainfall events. L_e increased rapidly in response to rainfall during the dry-wet season transition in October and increased consistently during the beginning of the wet season to values that exceeded $120 \text{ J m}^{-2} \text{ s}^{-1}$ by February 2012 (Figure 7a). The seasonal variations in L_e are larger and more dynamic than those observed for tropical and transitional forest [Malhi et al., 2002; Vourlitis et al., 2008; da Rocha et al., 2009] but are comparable to those observed for cerrado [da Rocha et al., 2002; Santos et al., 2003; Oliveira et al., 2005; Giambelluca et al., 2009].

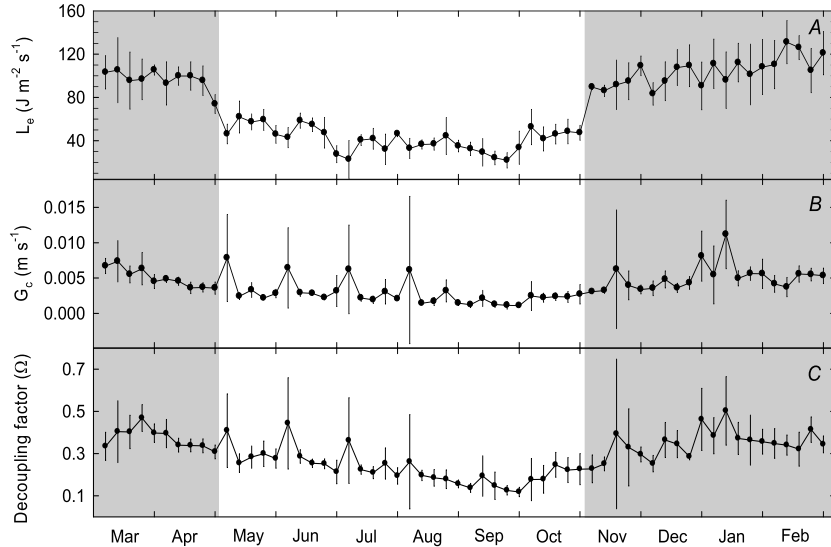


Figure 7. (a) Average weekly ($\pm\text{sd}$) latent heat flux, (b) canopy conductance, and (c) the decoupling factor. Shaded portions indicate the wet season.

[28] Smaller variations were observed for weekly average G_c (Figure 7b) and Ω (Figure 7c) during the study period. G_c ranged between 0.005 and 0.0075 m s^{-1} during the March–April 2011 wet season and declined into the dry season in May–September (Figure 7b). However, transient increases in G_c occurred throughout the dry season in response to cold fronts [Machado et al., 2004] that brought rain, wind, and colder temperatures to the region (see Figure 4). The wet season values of G_c are similar to those reported for tropical transitional forest [Vourlitis et al., 2008] but approximately 40–50% lower than those reported for humid evergreen tropical forest [da Rocha et al., 2004]. However, our dry-season values are comparable to other grass-dominated cerrado sites [Giambelluca et al., 2009] and reflect the more extreme drought and lower physiological activity that occurs with cerrado trees and grasses during the dry season [Santos et al., 2004; Vourlitis and da Rocha, 2011; Dalmagro et al., 2013]. Ω was on average 0.48 during the wet season and declined to a minimum value of 0.21 by the end of September (Figure 7c), which corresponds to the seasonal variation in D (Figure 4c).

[29] Cerrado also displays a larger and faster response to variations in rainfall than transitional and humid tropical forest, especially during the dry season when drought stress is at a seasonal maximum [Giambelluca et al., 2009]. These large but transient increases in L_e and G_c appear to be driven by rapid evaporation in response to rainfall. To assess the response to cerrado to rainfall pulses, we selected a period during the dry (October, days 274–278) and wet (January, days 23–28) seasons where there was a rainfall event of 10 and 45 mm, respectively. R_n was similar before and after these rainfall events in both the dry (Figure 8a) and wet (Figure 8b) seasons. However, during the dry season, D was substantially higher before the rainfall pulse compared to after (Figure 8c) while L_e and G_c were substantially higher after the rainfall pulse (Figures 8e and 8g). During this time the EVI was at a seasonal minimum (Figure 5) and physiological activity of cerrado grasses and trees are also low due to prolonged drought [Santos et al., 2004; Vourlitis and

da Rocha, 2011; Dalmagro et al., 2013], thus the increase in L_e and G_c in response to the dry-season rainfall pulse is presumably due almost entirely to evaporation. Such large responses in mass exchange are more comparable to semiarid (i.e., chaparral; [Luo et al., 2007]) and arid (desert; [Hastings et al., 2005]) ecosystems and highlight the importance of rainfall pulses that occur after prolonged periods of drought. In contrast, no such variations were observed during the wet season (Figures 8d, 8f, and 8h), even though the rainfall event was 4 times higher during the wet season. During the wet season, EVI is at a seasonal maximum and trees and grasses are physiologically active, and rainfall pulses act to increase surface and soil water content, which is already adequate to support high rates of evaporation and transpiration [Santos et al., 2004; Giambelluca et al., 2009; Vourlitis and da Rocha, 2011; Dalmagro et al., 2013]. Thus, rainfall pulses during the wet season have little effect on rates of L_e and G_c .

3.5. Direct and Indirect Controls on L_e and G_c

[30] Path analysis was used to quantify the direct and indirect effects of meteorology (R_n , D , T_a), water availability (P and SH_2O), and phenology (EVI) on L_e and G_c (Figure 2). Our data indicate that L_e was significantly and positively affected by SH_2O and R_n and negatively affected by D (Table 1), which is consistent with the data reported here and from other studies of cerrado and tropical forest L_e [da Rocha et al., 2002, 2009; Malhi et al., 2002; Santos et al., 2003; Oliveira et al., 2005; Vourlitis et al., 2008; Giambelluca et al., 2009].

[31] For G_c , path analysis revealed a more complex interaction between the meteorological variables (Table 1). For example, there was a significant direct negative effect of R_n and D on G_c and a significant positive direct effect of T_a on G_c (Table 1). The negative effect of D on G_c is expected given the close coupling of the canopy and atmosphere and the importance of D on stomatal conductance [Bucci et al., 2008; Vourlitis and da Rocha, 2011; Dalmagro et al., 2013]. However, the negative effect of R_n is surprising, but upon closer inspection, the peaks in G_c

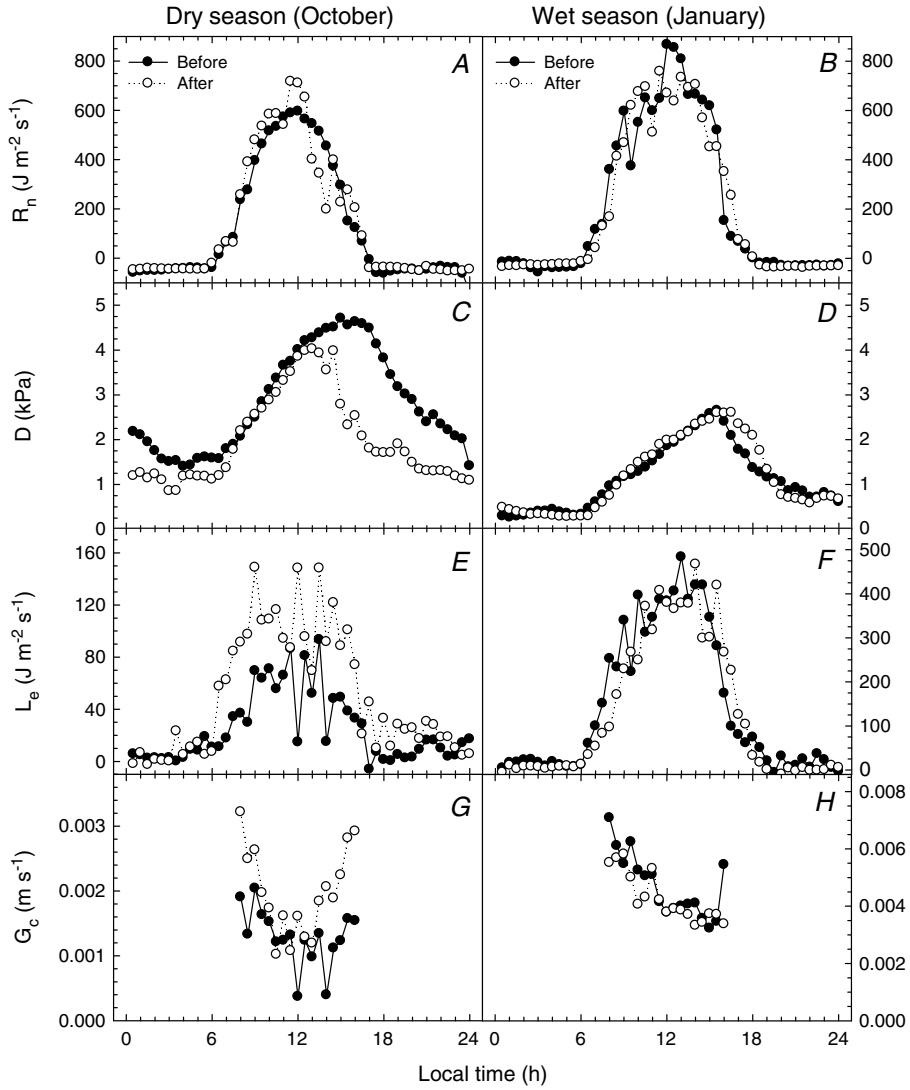


Figure 8. (a and b) Average diel trends in net radiation, (c and d) vapor pressure deficit, (e and f) latent heat flux, and (g and h) canopy conductance for periods before (closed symbols) and after (open symbols) a rainfall event that occurred during the dry season in Figures 8a, 8c, 8e, and 8g and the wet season in Figures 8b, 8d, 8f, and 8h.

observed during the study period (i.e., the weeks of 10 May, 14 June, 19 July, and 23 August; Figure 7b) were associated with short-term cold fronts that also reduced R_n (see Figure 4). If these points are removed, the relationship between R_n and G_c becomes positive, which is expected from previous research and theory [Dolman *et al.*, 1991; Harris *et al.*, 2004]. Another interesting result was the positive direct relationship between T_a and G_c (Table 1). Again, one would assume that an increase in T_a would lead to a direct increase in D and a decline in G_c ; however, when averaged by season, both T_a and G_c were higher during the wet season and lower during the dry season (see Figures 4c and 7b), which presumably accounts for the positive relationship.

[32] All of the indirect effects on G_c , with the exception of R_n , were smaller than the direct effects, and therefore, likely to not be significant. However, the indirect effects of P and SH_2O on G_c were larger, and opposite in sign, than the direct effects.

Table 1. Path Coefficients of the Direct and Indirect Effects of Average Weekly Precipitation (P), Net Radiation (R_n), Soil Moisture Content (SH_2O), Air Temperature (T_a), Vapor Pressure Deficit (D), and the Enhanced Vegetation Index (EVI) on Average Weekly Latent Heat Flux (L_e) and Canopy Conductance (G_c)^a

Variable	L_e		G_c	
	Direct	Indirect	Direct	Indirect
EVI	-0.001	NA	0.393	NA
P	0.032	0.044	0.052	-0.411
R_n	0.976	-0.133	-0.820	-1.229
SH_2O	0.282	0.209	-0.053	0.852
T_a	-0.051	-0.272	2.228	-1.103
D	-0.288	<0.001	-0.991	-0.023

^aBold values indicate statistically significant ($p < 0.05$) coefficients, determined using multiple-linear regression and only correspond to the direct effects of each variable on L_e or G_c . NA = not applicable.

Table 2. Estimates of the Total Annual Precipitation (P) and the Average Latent Heat Flux (L_e) for the Dry and Wet Seasons and Over Annual Periods^a

Site ID ^b Type	P (mm/y)	Average L_e			Difference (Dry-Wet) (%)	Reference
		Dry	Wet ($\text{J m}^{-2} \text{s}^{-1}$)	Annual		
K34-AF	2286	98	81	90	21	<i>da Rocha et al. [2009]</i>
CUE-AF	2089	79	96	87	17	<i>Malhi et al. [2002]</i>
K67-AF	1863	85	76	80	12	<i>Hutyra et al. [2005]</i>
K67-AF	1736	87	73	80	18	<i>Hutyra et al. [2005]</i>
K67-AF	2314	86	76	81	14	<i>Hutyra et al. [2005]</i>
K67-AF	2494	93	71	82	32	<i>Hutyra et al. [2005]</i>
K83-AF	1811	114	103	109	11	<i>da Rocha et al. [2004]</i>
JRU-AF	2173	109	105	107	4	<i>von Randow et al. [2004]</i>
SIN-TF	1999	71	74	72	4	<i>Vourlitis et al. [2002, 2008]</i>
SIN-TF	2161	79	77	78	3	<i>Vourlitis et al. [2002, 2008]</i>
SIN-TF	2006	71	77	74	9	<i>Vourlitis et al. [2002, 2008]</i>
SIN-TF	1861	74	77	75	4	<i>Vourlitis et al. [2002, 2008]</i>
SIN-TF	2253	66	61	64	8	<i>Vourlitis et al. [2002, 2008]</i>
SIN-TF	2040	87	80	83	9	<i>Vourlitis et al. [2002, 2008]</i>
BAN-TF	1692	90	113	101	20	<i>Borma et al. [2009]</i>
BAN-TF	1471	91	102	97	10	<i>Borma et al. [2009]</i>
BAN-TF	1914	80	115	97	31	<i>Borma et al. [2009]</i>
PEG-Css	1478	39	88	64	56	<i>da Rocha et al. [2002]</i>
FM-Ccs	1030	43	100	72	57	This study
FM-Ccs	1415	41	78	59	48	<i>Rodrigues et al. [2013]</i>
FM-Ccs	1353	40	84	62	52	<i>Rodrigues et al. [2013]</i>
IGB-Ccs	1017	47	88	68	46	<i>Santos et al. [2003]</i>
IGB-Cd	1504	53	119	86	56	<i>Oliveira et al. [2005]</i>
IGB-Ccs	1504	29	108	69	73	<i>Oliveira et al. [2005]</i>
IGB_Cd	1440	53	68	62	23	<i>Giambelluca et al. [2009]</i>
IGB_Cc	1440	40	56	49	28	<i>Giambelluca et al. [2009]</i>
IGB_Cd	1440	54	75	66	27	<i>Giambelluca et al. [2009]</i>
IGB_Cc	1440	41	69	58	40	<i>Giambelluca et al. [2009]</i>
PAN-GF	1414	71	113	92	38	<i>Sanches et al. [2011]</i>

^aEstimates include the data collected in this study (see the bold values in the table) and data reported in the literature. Site information includes the vegetation type (AF = Amazonian humid evergreen forest, TF = transitional forest, Css = Cerrado sensu stricto, Ccs = Cerrado campo sujo, Cd = Cerrado denso, Cc = Cerrado campo, and GF = gallery forest). Also shown is the percentage change in L_e from wet to the dry season calculated as $((\text{Dry } L_e - \text{Wet } L_e)/\text{Wet } L_e) * 100$.

^bK34 = Manaus, AM (K34); CUE = Manaus, AM (Cueiras); K67 = Santarem, PA (K67); K83 = Santarem, PA (K83), SIN = Sinop, MT; BAN = Banala Island, TO; PEG = Pe de Gigante, SP; FM = Fazenda Miranda, MT; IGB = Instituto Brasileiro de Geografia e Estatística (IBGE) Ecological Reserve, DF; and PAN = Pantanal, MT.

In terms of P , the effect was negative, but for SH_2O , the effect was positive, which seems hard to explain. However, rainfall events are short-term phenomena, and during these events, surface water availability increases rapidly, R_n declines because of cloud cover, and G_c increases. After the rainfall event, SH_2O increases, and because of the water holding capacity of soil, surface water availability remains high for a longer period of time, this leading to an increase in G_c . This is especially true during the dry-season rainfall pulses, when an increase in L_e and G_c can occur over several days after a rainfall event (Figure 8).

[33] We also hypothesized that EVI would significantly and positively affect L_e ; however, path analysis failed to reveal any significant direct or indirect effects of the EVI on L_e or G_c (Table 1). This result was surprising given that EVI was significantly positively correlated with L_e ($r=0.74$; $p < 0.001$) and G_c ($r=0.61$; $p < 0.001$), but ultimately, the reason why the EVI was not found to directly affect L_e or G_c was that all three variables (EVI, L_e , and G_c) were either directly or indirectly affected by surface water availability. For example, both the EVI and L_e were positively directly affected by variations in SH_2O , while G_c was positively indirectly affected by SH_2O through its control

on D . While EVI (or leaf area) is an important control on L_e and G_c [Vourlitis et al., 2008; Giambelluca et al., 2009; Yerba et al., 2013], variations in surface water availability ultimately controlled temporal variations in EVI, L_e , and G_c .

3.6. Comparisons to Other Studies

[34] Our data reveal large seasonal variations in energy flux variables, but unfortunately, our study period only encompassed one year, which precludes an assessment of interannual variations in energy balance and limits our ability to generalize our results to other campo-type cerrado ecosystems. To determine how “representative” our data are to other tropical ecosystems, we surveyed the literature to assess how L_e varied within cerrado ecosystems and between other tropical ecosystems such as transitional and humid evergreen forest (see site locations in Figure 1). The data (Table 2) span multiple sites and/or years and to our knowledge, are the most exhaustive summary of L_e for Brazilian tropical ecosystems to date. These data indicate that the dry and wet season rates of L_e reported here are comparable to those reported for other cerrado ecosystems even though annual rainfall was approximately 400 mm less than the long-term average for the region. Furthermore, the seasonal variation that we describe here is typical of other

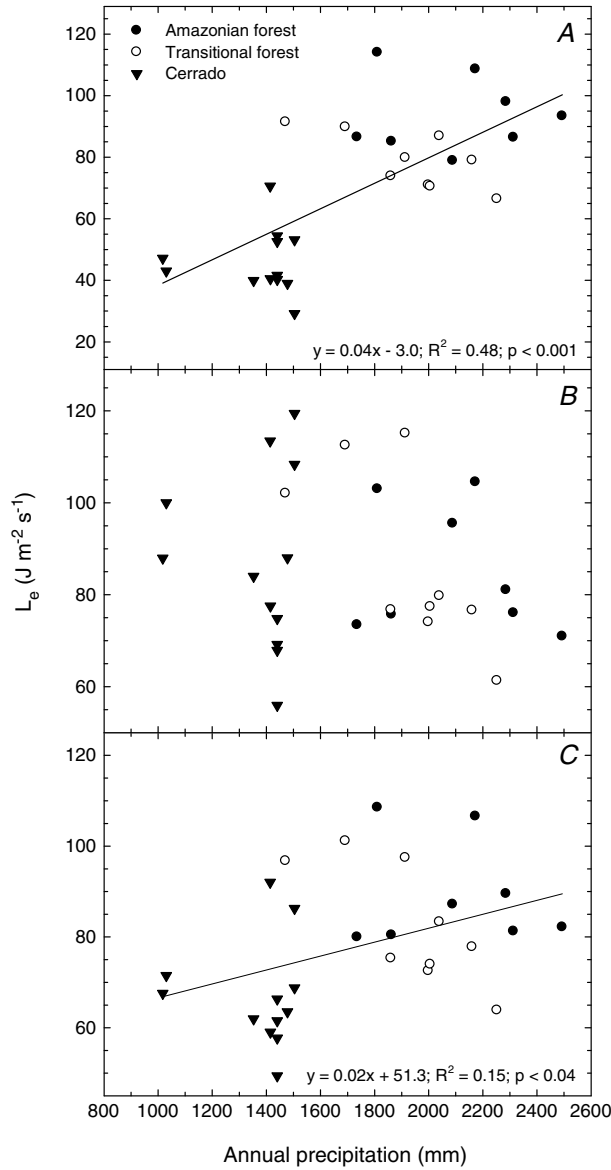


Figure 9. Estimates of (a) dry season, (b) wet season, and (c) average annual latent heat flux as a function of average annual precipitation from this study and from Amazonian humid evergreen forests (black circles), transitional forests (white circles), and cerrado (inverted triangles) reported in the literature (see Table 2 for data sources and Figure 1 for approximate site locations). Significant linear trends are depicted with the line and equation of best fit, coefficient of determination (R^2), and the probability that the line is significantly different from zero (p).

cerrado stands but substantially less than transitional and humid tropical forests (Table 2).

[35] Other patterns emerge when data displayed in Table 2 are graphed as a function of average annual rainfall (Figure 9). First, dry-season rates of L_e increased significantly as a function of average annual rainfall (Figure 9a), because wetter sites have higher water availability and/or a shorter duration in the length of the dry season [Vourlitis et al., 2005; da Rocha et al., 2009; Costa et al., 2010]. In contrast, wet season rates of L_e were insensitive to variations in annual rainfall indicating that

cerrado, transitional forest, and Amazonian forests have similar rates of L_e provided that surface soil water availability is adequate. Furthermore, wetter sites typically have more frequent cloud cover, especially during the wet season, which reduces available energy (R_n), and thus, L_e [Malhi et al., 2002; da Rocha et al., 2009; Costa et al., 2010]. Over an annual cycle, L_e is found to increase as a function of average annual rainfall because of the dry-season water limitations observed in the drier, more seasonal cerrado sites (Figure 9c).

[36] The discussion above illustrates the importance of precipitation amount and timing on seasonal and annual patterns of L_e , but in cerrado, similar variations may be observed between arboreal and grass-dominated forms of cerrado. For example, tree-dominated cerrado, such as the Cambarazal site in the Pantanal (PAN; Table 2), exhibits smaller seasonal variations in L_e that are similar to that observed for transitional forest [Vourlitis and da Rocha, 2011]. The lower variation in L_e for forested cerrado is due to more consistent leaf area index (LAI) [Ratana et al., 2005] and deeper rooting depth [Oliveira et al., 2005; Sanches et al., 2011]. Cerrado with higher shrub and tree cover, such as *denso* and *sensu stricto* forms, typically have higher rates of wet season and annual L_e than grass-dominated *campo* cerrado (Table 2) [Oliveira et al., 2005; Giambelluca et al., 2009]. These within biome variations in energy flux density are affected by stand structural characteristics, such as tree density and cover, LAI, and rooting depth [Oliveira et al., 2005; Giambelluca et al., 2009], which in turn may be affected more by soil chemistry and physical properties and/or disturbance regimes [Eiten, 1972; de Assis et al., 2011; Vourlitis et al., 2013], than by the timing and/or amount of rainfall. Similar structural controls on L_e are likely operating across the Amazonian forest-cerrado gradient described here (Table 2 and Figure 9); however, over this larger spatial scale, variations in stand structure are highly correlated with rainfall timing and/or amount [Keller et al., 2004; Machado et al., 2004; Saleska et al., 2009].

4. Conclusions

[37] Energy fluxes were measured using eddy covariance from March 2011–2012 in a mixed grassland (*campo sujo*) in south central Mato Grosso, Brazil. As we hypothesized, our data indicate that seasonal variation in precipitation and/or surface water availability was the most important variable controlling energy fluxes and canopy conductance. Seasonal variation in soil water availability (SH_2O) was a key control on G_c , and the high surface-atmosphere coupling (i.e., low Ω) indicated that variation in stomatal conductance may have been the most important control on rates of G_c , especially during the dry season when water stress limits stomatal conductance. G_c , L_e , and Ω exhibited rapid and dynamic responses to rainfall pulses that were qualitatively similar to those observed from arid and semiarid ecosystems.

[38] Such large seasonal variations were typical for many cerrado ecosystems, but as annual rainfall increased, seasonal variations in L_e diminished. For example, estimates of L_e described here and in the literature indicate that dry-season rates of L_e are positively correlated with average annual rainfall, because water limitations decline in wetter areas. In contrast, wet season rates of L_e are insensitive to average annual rainfall because of a release of drought limitations in water-limited systems (cerrado) and more intense and/or frequent

cloud cover in wetter areas. Over an annual basis, average L_e increases significantly across the approximately 1400 mm rainfall gradient in tropical Brazil because of the strong dry-season water limitations to L_e in cerrado, and to a lesser extent, transitional tropical forest.

[39] Our data indicate a high sensitivity of cerrado energy balance to seasonal variations in rainfall. Land cover and climate change are expected to lead to an increase in the dry-season duration and a decrease in rainfall. The high-sensitivity energy partitioning to water availability in the grass-dominated cerrado studied here, and other cerrado ecosystems reported in the literature, has important implications to local and regional energy balance.

[40] **Acknowledgments.** The research was supported by the Universidade Federal de Mato Grosso (UFMT), Programa de Pós Graduação em Física Ambiental (PPGFA) IF/UFMT, Grupo de Ecofisiologia Vegetal (GPEV), Coordenação de Aperfeiçoamento de Pessoal do Ensino Superior (CAPES), the U.S. National Science Foundation-Office of International Science and Engineering (NSF-OISE), and the Projeto Ciência sem Fronteira (Science Without Border), projeto 120/2012 CAPES/CNPQ. Special thanks to Clovis Miranda and his family for allowing this work to be conducted at Fazenda Miranda.

References

- Araújo, A. C., et al. (2002), Comparative measurements of carbon dioxide fluxes from two nearby towers in a central Amazonia rainforest: The Manaus LBA site, *J. Geophys. Res.*, **107**(D20), 8090, doi:10.1029/2001JD000676.
- Aubinet, M., et al. (2000), Estimates of the annual net carbon and water exchange of forests: The EUROFLUX methodology, *Adv. Ecol. Res.*, **30**, 113–175, doi:10.1016/S0065-2504.
- Bagayoko, F., S. Yonkeu, J. Elbers, and N. Van de Giesen (2007), Energy partitioning over the West African savanna: Multi-year evaporation and surface conductance measurements in Eastern Burkina Faso, *J. Hydrol.*, **334**, 545–559, doi:10.1016/j.jhydrol.2006.10.035.
- Baidya Roy, S., and R. Avissar (2002), Impact of land use/land cover change on regional hydrometeorology in Amazonia, *J. Geophys. Res.*, **107**, D20, 8037, doi:10.1029/2000JD000266.
- Baldocchi, D. D., R. J. Luxmoore, and J. L. Hatfield (1991), Discerning the forest from the trees: An essay of scaling canopy stomatal conductance, *Agric. For. Meteorol.*, **54**, 197–226, doi:10.1016/0168-1923(91)90006-C.
- Biudes, M. S. (2008), Balanço de energia em área de vegetação monodominante de Cambará e pastagem no norte do Pantanal. Thesis (doutorado)—Universidade Federal de Mato Grosso, Faculdade de Agronomia e Medicina Veterinária, Pós-graduação em Agricultura Tropical.
- Borma, L. S., et al. (2009), Atmospheric and hydrological controls of the evapotranspiration over a floodplain forest in the Bananal Island region, Amazonia, *J. Geophys. Res.*, **114**, G01003, doi:10.1029/2007JG000641.
- Bucci, S. J., F. G. Scholz, G. Goldstein, F. C. Meinzer, A. C. Franco, Y. Zhang, and G. Y. Hao (2008), Water relations and hydraulic architecture in Cerrado trees: Adjustments to seasonal changes in water availability and evaporative demand, *Braz. J. Plant Physiol.*, **20**(3), 233–245, doi:10.1590/S1677-04202008000300007.
- Costa, M. H., and G. F. Pires (2010), Effects of Amazon and Central Brazil deforestation scenarios on the duration of the dry season in the arc of deforestation, *Int. J. Climatol.*, **30**, 1970–1979, doi:10.1002/joc.2048.
- Costa, M. H., M. C. Biajoli, L. Sanches, A. C. M. Malhado, L. R. Hutyra, H. R. da Rocha, R. G. Aguiar, and A. C. de Araújo (2010), Atmospheric versus vegetation controls of Amazonian tropical rain forest evapotranspiration: Are the wet and seasonally dry rain forests any different?, *J. Geophys. Res.*, **115**, G04021, doi:10.1029/2009JG001179.
- Culf, A. D., J. L. Esteves, A. de O. Marques Filho, and H. R. da Rocha (1996), Radiation, temperature and humidity over forest and pasture in Amazonia, in *Amazonian Climate and Deforestation*, edited by J. H. C. Gash et al., pp. 175–192, J. M. Wiley, New York, NY, USA.
- da Rocha, H. R., H. C. Freitas, R. Rosolem, R. I. N. Juárez, R. N. Tannus, M. A. Ligo, O. M. R. Cabral, and M. A. F. Silva Dias (2002), Measurements of CO₂ exchange over a woodland savanna (Cerrado Sensu stricto) in southeast Brazil, *Biota Neotropica*, **2**, 1–11.
- da Rocha, H. R., et al. (2009), Patterns of water and heat flux across a biome gradient from tropical forest to savanna in Brazil, *J. Geophys. Res.*, **114**, G00B12, doi:10.1029/2007JG000640.
- Dalmagro, H. J., F. A. Lobo, G. L. Vourlitis, Á. C. Dalmolin, M. Z. Antunes Jr., C. E. R. Ortiz, and J. S. Nogueira (2013), Photosynthetic parameters for two invasive tree species of the Brazilian Pantanal in response to seasonal flooding, *Photosynthetica*, **51**, 281–294, doi:10.1007/s11099-013-0024-3.
- de Assis, A. C. C., R. M. Coelho, E. S. Pinheiro, and G. Durigan (2011), Water availability determines physiognomic gradient in an area of low-fertility soils under Cerrado vegetation, *Plant Ecol.*, **212**, 1135–1147, doi:10.1007/s11258-010-9893-8.
- Dolman, A., J. Gash, J. Roberts, and W. Shuttleworth (1991), Stomatal and surface conductance of tropical rainforest, *Agric. For. Meteorol.*, **54**, 303–318, doi:10.1016/0168-1923.
- Douglas, E. M., A. Beltrán-Przekurat, D. Niogi, R. A. Pielke Sr., and C. J. Vorosmarty (2009), The impact of agricultural intensification and irrigation on land-atmosphere interactions and Indian monsoon precipitation: A mesoscale modeling perspective, *Global Planet. Change*, **67**(1e2), 117–128, doi:10.1016/j.gloplacha.2008.12.007.
- Edwards, D., and B. C. Coull (1987), Autoregressive trend analysis: An example using long-term ecological data, *Oikos*, **50**, 95–102.
- Eiten, G. (1972), The cerrado vegetation of Brazil, *Bot. Rev.*, **38**, 201–341.
- Fisher, R. A., M. Williams, M. de Lourdes Ruivo, A. L. de Costa, and P. Meir (2008), Evaluating climatic and soil water controls on evapotranspiration at two Amazonian rainforest sites, *Agric. For. Meteorol.*, **148**, 850–861, doi:10.1016/j.agrformet.2007.12.001.
- Foley, J. A., M. H. Costa, C. Delire, N. Ramankutty, and P. Snyder (2003), Green Surprise? How terrestrial ecosystems could affect earth's climate, *Frontiers Ecol. Environ.*, **1**, 38–44, doi:10.1890/1540-9295.
- Furley, P. A., and J. A. Ratter (1988), Soil resources and plant communities of the central Brazilian cerrado and their development, *J. Biogeogr.*, **15**, 97–108.
- Giambelluca, T. W., F. G. Scholz, S. J. Bucci, F. C. Meinzer, G. Goldstein, W. A. Hoffmann, A. C. Franco, and M. P. Buchert (2009), Evapotranspiration and energy balance of Brazilians savannas with contrasting tree density, *Agric. For. Meteorol.*, **149**, 1365–1376, doi:10.1016/j.agrformet.2009.03.006.
- Grace, J., Y. Malhi, J. Lloyd, J. McIntyre, A. C. Miranda, P. Meir, and H. S. Miranda (1996), The use of eddy covariance to infer the net carbon dioxide uptake of Brazilian rain forest, *Global Change Biol.*, **2**, 209–217, doi:10.1111/j.1365-2486.1996.tb00073.x.
- Harris, P. P., C. Huntingford, P. M. Cox, J. H. C. Gash, and Y. Malhi (2004), Effect of soil moisture on canopy conductance of Amazonian rainforest, *Agric. For. Meteorol.*, **122**, 215–227, doi:10.1016/j.agrformet.2003.09.006.
- Hastings, S. J., W. C. Oechel, and A. Muhlia-Melo (2005), Diurnal, seasonal and annual variation in the net ecosystem CO₂ exchange of a desert shrub community (Sarcocaulaceous) in Baja California, Mexico, *Global Change Biol.*, **11**, 927–939, doi:10.1111/j.1365-2486.2005.00951.x.
- Hutyra, L. R., J. W. Munger, C. A. Nobre, S. R. Saleska, S. A. Vieira, and S. C. Wofsy (2005), Climatic variability and vegetation vulnerability in Amazonia, *Geophys. Res. Lett.*, **32**, L24712, doi:10.1029/2005GL024981.
- Huxman, T. E., A. A. Turnipseed, J. P. Sparks, P. C. Harley, and R. K. Monson (2003), Temperature as a control over ecosystem CO₂ fluxes in a high-elevation, subalpine forest, *Oecologia*, **134**, 537–546, doi:10.1007/s00442-002-1131-1.
- Jarvis, P. G., and K. G. McNaughton (1986), Stomatal control of transpiration: Scaling up from leaf to region, *Adv. Ecol. Res.*, **15**, 1–48.
- Jones, H. G. (1992), *Plants and Microclimate*, 2nd ed., 428 pp., Cambridge Univ. Press, Cambridge.
- Keller, M., et al. (2004), Ecological research in the large-scale biosphere-atmosphere experiment in Amazonia (LBA): Early results, *Ecol. Appl.*, **14**, S3–S16, doi:10.1890/03-6003.
- Klink, C. A., and A. G. Moreira (2002), Past and current human occupation and land-use, in *The Cerrados of Brazil: Ecology and Natural History of a Neotropical Savanna*, pp. 69–88, Columbia University Press, New York, USA.
- Lascano, R. J. (1991), Review of models for predicting soil water balance, in *Soil Water Balance in the Sudano-Sahelian Zone*, pp. 443–458, IAHS Press, Wallingford, Oxfordshire, OX10 8BB, UK.
- Lenza, E., and C. A. Klink (2006), Comportamento fenológico de espécies lenhosas em um cerrado sentido restrito de Brasília, DF, *Rev. Brasileira Botânica*, **29**, 627–638.
- Luo, H., W. C. Oechel, S. J. Hastings, R. Zulueta, Y. Qian, and H. Kwon (2007), Mature semiarid chaparral ecosystems can be a significant sink for atmospheric carbon dioxide, *Global Change Biol.*, **13**, 386–396, doi:10.1111/j.1365-2486.2006.01299.x.
- Machado, L. A. T., H. Laurent, N. Dessay, and I. Miranda (2004), Seasonal and diurnal variability of convection over the Amazonia: A comparison of different vegetation types and large scale forcing, *Theor. Appl. Climatol.*, **78**(1–3), 61–77, doi:10.1007/s00704-004-0044-9.

- Malhi, Y., E. Pegoraro, A. Nobre, J. Grace, A. Culf, and R. Clement (2002), Energy and water dynamics of a central Amazonian rain forest, *J. Geophys. Res.*, 107(D20), 8061, doi:10.1029/2001JD000623.
- Mantovani, W., and F. R. Martins (1988), Variáveis fenológicas das espécies de cerrado da Reserva biológica de Mogi Guaçu. Estado de São Paulo, *Rev. Brasileira Botânica*, 11, 101–112.
- McMillen, R. T. (1988), An eddy correlation technique with extended applicability to non-simple terrain, *Boundary Layer Meteorol.*, 43, 231–245, doi:10.1007/BF00128405.
- Miranda, A. C., H. S. Miranda, J. Lloyd, J. Grace, R. J. Francey, J. A. McIntyre, P. Meir, P. Riggan, R. Lockwood, and J. Brass (1997), Fluxes of carbon, water and energy over Brazilian cerrado: An analysis using eddy covariance and stable isotopes, *Plant Cell Environ.*, 20(3), 315–328, doi:10.1046/j.1365-3040.
- Monteith, J. (1981), Evaporation and surface temperature, *Q. J. R. Meteorol. Soc.*, 107, 1–27.
- Mueller, C. (2003), Expansion and modernization of agriculture in the cerrado—the case of soybeans in Brazil's center-west, Working Paper 306, Department of Economics, University of Brasilia, Brasilia.
- Niyogi, D., S. Raman, and K. Alapaty (1999), Uncertainty in specification of surface characteristics. Part 2: Hierarchy of interaction-explicit statistical analysis, *Boundary Layer Meteorol.*, 91, 341–366, doi:10.1023/A:1002023724201.
- Oak Ridge National Laboratory-Distributed Active Archive Center (ORNL-DAAC) (2013), http://daac.ornl.gov/cgi-bin/MODIS/GR_col5_1/mod_viz.html. Accessed June, 2011.
- Oliveira, R. S., L. Bezerra, E. A. Davidson, F. Pinto, C. A. Klink, D. C. Nepstad, and A. Moreira (2005), Deep root function in soil water dynamics in cerrado savannas of central Brazil, *Funct. Ecol.*, 19, 574–581, doi:10.1111/j.1365-2435.2005.01003.x.
- Pielke, R. A., Sr. (2001), Influence of the spatial distribution of vegetation and soils on the prediction of cumulus convective rainfall, *Rev. Geophys.*, 39(2), 151–177, doi:10.1029/1999RG000072.
- Pielke, R. A., Sr., et al. (2007), Unresolved issues with the assessment of multi-decadal global land surface temperature trends, *J. Geophys. Res.*, 112, D24S08, doi:10.1029/2006JD008229.
- Radambrasil (1982), Levantamentos dos recursos naturais ministério das minas de energia. Secretaria Geral. Projeto RADAMBRASIL. Folha SD 21 Cuiabá, Rio de Janeiro.
- Ratana, T., A. R. Huete, and L. Ferreira (2005), Analysis of cerrado physiognomies and conversion in the MODIS seasonal-temporal domain, *Earth Interact.*, 9(3), 1–22.
- Ray, D. K., U. S. Nair, R. M. Welch, Q. Han, J. Zeng, W. Su, T. Kikuchi, and T. J. Lyons (2003), Effects of land use in Southwest Australia: 1. Observations of cumulus cloudiness and energy fluxes, *J. Geophys. Res.*, 108(D14), 4414, doi:10.1029/2002JD002654.
- Rodrigues, T. R., L. F. A. Curado, J. W. Z. Novais, A. G. de Oliveira, S. R. Paulo, M. S. Biudes, and J. S. Nogueira (2011), Distribuição dos componentes do balanço de energia do Pantanal Mato-grossense, *Rev. Ciências Agro Ambientais* (Online), 9(2), 165–175.
- Rodrigues, T. R., S. R. de Paulo, J. W. Z. Novais, L. F. A. Curado, J. S. Nogueira, R. G. de Oliveira, F. A. Lobo, and G. L. Vourlitis (2013), Temporal patterns of energy balance for a Brazilian tropical savanna under contrasting seasonal conditions, *Int. J. Atmos. Sci.*, 326010, 9, doi:10.1155/2013/326010.
- Saleska, S., H. R. da Rocha, B. Krujt, and A. Nobre (2009), Ecosystem carbon fluxes and Amazonian forest metabolism, *Amazonia and Global Change, Geophysical Monograph Series*, 186, 389–408, Washington, D. C., doi:10.1029/2008GM000728.
- San José, J. J., N. Nikanova, and R. Bracho (1998), Comparison of factors affecting water transfer in a cultivated paleotropical grass (Brachiaria decumbens Stapf) field and a neotropical savanna during the dry season of the Orinoco lowlands, *Am. Meteorol. Soc.*, 33, 508–522, doi:10.1175/1520-0450.
- Sanches, L., G. L. Vourlitis, M. C. Alves, O. B. Pinto-Júnior, and J. S. Nogueira (2011), Seasonal patterns of evapotranspiration for a Vochysia divergens forest in the Brazilian Pantanal, *Wetlands*, 3, 1215–1225, doi:10.1007/s13157-011-0233-0.
- Santos, A. J. B., G. T. D. A. Silva, H. S. Miranda, A. C. Miranda, and J. Lloyd (2003), Effects of fire on surface carbon, energy and water vapour fluxes over campo sujo savanna in central Brazil, *Funct. Ecol.*, 17, 711–719, doi:10.1111/j.1365-2435.2003.00790.x.
- Santos, A. J. B., C. A. Quesada, G. T. da Silva, J. F. Maia, H. S. Miranda, A. C. Miranda, and J. Lloyd (2004), High rates of net ecosystem carbon assimilation by Brachiaria pasture in the Brazilian Cerrado, *Global Change Biol.*, 10, 77–885, doi:10.1111/j.1529-8817.2003.00777.x.
- Scholes, R. J., and S. R. Archer (1997), Tree-grass interactions in Savannas, *Annu. Rev. Ecol. Syst.*, 28, 517–544.
- Schuepp, P. H., M. Y. Leclerc, J. I. MacPherson, and R. L. Desjardins (1990), Footprint prediction of scalar fluxes from analytical solutions of the diffusion equation, *Boundary Layer Meteorol.*, 50, 355–373, doi:10.1007/BF00120530.
- Silvério, D. V., and E. Lenza (2010), Fenologia de espécies lenhosas em um cerrado típico no Parque Municipal do Bacaba, Nova Xavantina, Mato Grosso, Brasil, *Biota Neotropica*, 10, 205–216.
- Sokal, R. R., and F. J. Rohlf (1995), *Biometry*, 3rd ed., 887 pp., Freeman, San Francisco, Calif.
- Teepe, R., H. Dilling, and F. Beese (2003), Estimating water retention curves of forest soils from soil texture and bulk density, *J. Plant Nutr. Soil Sci.*, 166, 111–119.
- Von Randow, C., et al. (2004), Comparative measurements and seasonal variations in energy and carbon exchange over forest and pasture in South West Amazonia, *Theor. Appl. Climatol.*, 78, 5–26, doi:10.1007/s00704-004-0041-z.
- Vourlitis, G. L., N. Priante-Filho, M. M. S. Hayashi, J. de Sousa Nogueira, F. T. Caseiro, and J. H. Campelo Jr. (2002), Seasonal variations in the evapotranspiration of a transitional tropical forest of Mato Grosso, Brazil, *Water Resour. Res.*, 38(6, 1094), doi:10.1029/2000WR000122.
- Vourlitis, G. L., J. de S Nogueira, N. Priante-Filho, W. Hoeger, F. Raiter, M. S. Biudes, J. C. Arruda, V. B. Capistrano, J. L. B. de Faria, and F. de Almeida Lobo (2005), The sensitivity of diel CO₂ and H₂O vapor exchange of a tropical transitional forest to seasonal variation in meteorology and water availability, *Earth Interact.*, 9(27), 1–23, doi:10.1175/EI124.1.
- Vourlitis, G. L., J. de Souza Nogueira, F. de Almeida Lobo, K. M. Sendall, S. R. de Paulo, C. A. Antunes Dias, O. B. Pinto Jr., and N. L. R. de Andrade (2008), Energy balance and canopy conductance of a tropical semi-deciduous forest of the southern Amazon Basin, *Water Resour. Res.*, 44, W03412, doi:10.1029/2006WR005526.
- Vourlitis, G. L., F. A. Lobo, S. Lawrence, I. C. Lucena, O. P. Borges Jr., H. J. Dalmagro, C. E. R. Ortiz, and J. S. Nogueira (2013), Variations in stand structure and diversity along a soil fertility gradient in a Brazilian savanna (Cerrado) in southern Mato Grosso, *Soil Sci. Soc. Am. J.*, 1370–1379, doi:10.2136/sssaj2012.0336.
- Vourlitis, G. L., and H. R. da Rocha (2011), Flux dynamics in the cerrado and cerrado-forest transition of Brazil, in *Ecosystem Function in Global Savannas: Measurement and Modeling at Landscape to Global Scales*, edited by M. J. Hill and N. P. Hanan, pp. 97–116, CRC, Inc., Boca Raton, FL, USA.
- Webb, E. K., G. I. Pearman, and R. Leuning (1980), Corrections of flux measurements for density effects due to heat and water vapor transfer, *Q. J. R. Meteorol. Soc.*, 106, 85–100.
- Yerba, M., A. Van Dijk, R. Leuning, A. Huete, and J. P. Guerschman (2013), Evaluation of optical remote sensing to estimate actual evapotranspiration and canopy conductance, *Remote Sens. Environ.*, 129, 250–261, doi:10.1016/j.rse.2012.11.004.
- Zeri, M., and L. D. A. Sá (2010), The impact of data gaps and quality control filtering on the balances of energy and carbon for a Southwest Amazon forest, *Agric. For. Meteorol.*, 150, 1543–1552, doi:10.1016/j.agrformet.2010.08.004.